

Manuscript Number: MUTREV-D-09-00037R1

Title: Spatiotemporal characterization of ionizing radiation induced DNA damage foci and their relation to chromatin organization

Article Type: Special Issue: ESF-EMBO 2009

Keywords: DSB, γ H2AX, ATMp, 53BP1, repair kinetics, review, chromatin, complex damage

Corresponding Author: Dr. Sylvain V. Costes, Ph.D.

Corresponding Author's Institution: Lawrence Berkeley National Laboratory

First Author: Sylvain V Costes, Ph.D.

Order of Authors: Sylvain V Costes, Ph.D.; Irene Chiolo, Ph.D.; Janice M Pluth, Ph.D.; Mary Helen Barcellos-Hoff, Ph.D.; Burkhard Jakob, Ph.D.

Abstract: DNA damage sensing proteins have been shown to localize to the sites of DNA double strand breaks (DSB) within seconds to minutes following ionizing radiation (IR) exposure, resulting in the formation of microscopically visible nuclear domains referred to as radiation-induced foci (RIF). This review characterizes the spatio-temporal properties of RIF at physiological doses, minutes to hours following exposure to ionizing radiation, and it proposes a model describing RIF formation and resolution as a function of radiation quality and chromatin territories. Discussion is limited to RIF formed by three interrelated proteins ATM (Ataxia telangiectasia mutated), 53BP1 (p53 binding protein 1) and γ H2AX (phosphorylated variant histone H2AX), with an emphasis on the later. This review discusses the importance of not equating RIF with DSB in all situations and shows how dose and time dependence of RIF frequency is inconsistent with a one to one equivalence. Instead, we propose that RIF mark regions of the chromatin that would serve as scaffolds rigid enough to keep broken DNA from diffusing away, but open enough to allow the repair machinery to access the damage site. We review data indicating clear kinetic and physical differences between RIF emerging from dense and uncondensed regions of the nucleus. We suggest that persistent RIF observed days following exposure to ionizing radiation are nuclear marks of permanent rearrangement of the chromatin architecture. Such chromatin alterations may not always lead to growth arrest as they have been shown to be able to replicate. Thus, heritable persistent RIF spanning over tens of Mbp may reflect persistent changes in the transcriptome of a large progeny of cells. Such model opens the door to a "non-DNA-centric view" of radiation-induced phenotypes.

M. Lobrich, P. K. Cooper and B. Rydberg, Joining of correct and incorrect DNA ends at double-strand breaks produced by high-linear energy transfer radiation in human fibroblasts. *Radiat Res* 150, 619-626 (1998).

B. Stenerlow, E. Blomquist, E. Grusell, T. Hartman and J. Carlsson, Rejoining of DNA double-strand breaks induced by accelerated nitrogen ions. *Int J Radiat Biol* 70, 413-420 (1996).

P. F. Wilson, P. B. Nham, S. S. Urbin, J. M. Hinz, I. M. Jones and L. H. Thompson, Inter-individual variation in DNA double-strand break repair in human fibroblasts before and after exposure to low doses of ionizing radiation. *Mutat Res* (2009).

ABSTRACT

DNA damage sensing proteins have been shown to localize to the sites of DNA double strand breaks (DSB) within seconds to minutes following ionizing radiation (IR) exposure, resulting in the formation of microscopically visible nuclear domains referred to as radiation-induced foci (RIF). This review characterizes the spatio-temporal properties of RIF at physiological doses, minutes to hours following exposure to ionizing radiation, and it proposes a model describing RIF formation and resolution as a function of radiation quality and chromatin territories. Discussion is limited to RIF formed by three interrelated proteins ATM (Ataxia telangiectasia mutated), 53BP1 (p53 binding protein 1) and γ H2AX (phosphorylated variant histone H2AX), with an emphasis on the later. This review discusses the importance of not equating RIF with DSB in all situations and shows how dose and time dependence of RIF frequency is inconsistent with a one to one equivalence. Instead, we propose that RIF mark regions of the chromatin that would serve as scaffolds rigid enough to keep broken DNA from diffusing away, but open enough to allow the repair machinery to access the damage site. We review data indicating clear kinetic and physical differences between RIF emerging from dense and uncondensed regions of the nucleus. We suggest that persistent RIF observed days following exposure to ionizing radiation are nuclear marks of permanent rearrangement of the chromatin architecture. Such chromatin alterations may not always lead to growth arrest as they have been shown to be able to replicate. Thus, heritable persistent RIF spanning over tens of Mbp may reflect persistent changes in the transcriptome of a large progeny of cells. Such model opens the door to a “non-DNA-centric view” of radiation-induced phenotypes.

1

Costes et al.

1/21

2

3

4

Spatiotemporal characterization of ionizing radiation induced DNA damage foci and their relation to chromatin organization

5

6

7

8

9

10

11

S.V. Costes¹, I. Chiolo¹, J.M. Pluth¹, M.H. Barcellos-Hoff² and B. Jakob³

12

13

14

15

16

1. Life Sciences Division, Lawrence Berkeley National Laboratory, Berkeley, CA, USA

17

18

19

2. New York University School of Medicine, New York, NY, USA

20

21

22

3. GSI Helmholtzzentrum für Schwerionenforschung GmbH, Biophysik, Darmstadt,
Germany

23

24

25

26

27

28

29

30

Corresponding Author:

31

Sylvain V. Costes

32

33

Lawrence Berkeley National Laboratory

34

35

1 Cyclotron Road, MS: 977R225A

36

37

Berkeley, CA 94720

38

39

Tel: (510) 486-6988 / Fax: (510) 486-5586/ Email: svcostes@lbl.gov

40

41

42

43

44

45

46

47

48

49

50

51

52

Running title: Radiation induced foci and chromatin organization

53

54

55

56

57

58

59

60

61

62

63

64

65

Pages: 20

Word Count: 8,986

Fig.s: 4

Tables: 1

Key Words: DSB, γ H2AX, ATMp, 53BP1, repair kinetics, review, chromatin, complex damage

Abbreviations:

RIF: Radiation-induced foci

DSB: Double strand break

IR: Ionizing radiation

Post-IR: Following exposure to ionizing radiation

ATM: Ataxia telangiectasia mutated

ATMp: ATM phosphorylated at serine 1981

γ -H2AX: Histone H2AX phosphorylated at serine 139

53BP1: p53 Binding protein 1

PFGE: Pulse field gel electrophoresis

LET: Linear energy transfer (typical unit: keV/um)

HZE: Ions with high energy and high atomic number

9
10
11
12

13 Introduction

14
15
16
17
18
19
A well accepted paradigm in radiation biology is that ionizing radiation (IR)
induced DNA double strand breaks (DSB) are the most deleterious form of DNA
damage. It is thought that unrepaired DSB lead to death and misrepaired DSB may lead
to viable chromosomal rearrangements. Some of these rearrangements may be
instrumental in the development of cancer. DSB happen regularly in cells as
consequences of cell exposure to external insults or internal metabolism, such as,
oxidative stress or DNA replication errors. Thus cells have evolved efficient and rapid
repair responses to maintain the integrity of the genome. Sensor proteins are thought to
detect the presence of a DSB, and then recruit transducer proteins which provide the
signals to enzymes to repair the break. Depending on the severity of the damage and the
cell cycle status of the damaged cell, sensor proteins, also modified by transducers, will
induce either cell cycle delay for repair, programmed cell death or senescence.20
21
22
23
24
25
26
27
28
29
30
31
32
33
34
35
Sensor proteins have been shown to localize to the sites of DSB within seconds to
minutes following IR exposure, resulting in the formation of microscopically visible
nuclear domains referred to as radiation-induced foci (RIF). In mammalian cells, Rad51
protein was one of the first proteins identified as forming RIFs in mitotic and meiotic
cells (1, 2). Since then, many proteins have been shown to form RIFs and these proteins
can be divided into three categories: 1. proteins recruited to damage sites such as 53BP1
(3), MRE11 or NBS1 (4, 5); 2. proteins modification near the damage site, such as the
phosphorylation of H2AX (γ H2AX (6)); 3. foci resulting from both processes, such as the
RIF of phosphorylated (pS1981) ATM (Ataxia Telangiectasia Mutated) (7) and
phosphorylated (pT2609, pS2056) DNA-PKcs (8, 9). This review will limit its
discussion to three interrelated proteins ATM, 53BP1 and γ H2AX which form minutes
following IR. The relationship between RIF and chromatin organization will be discussed
with a primary emphasis on γ H2AX.36
37
38

39 Spontaneous foci

40
41
42
43
44
45
46
47
48
49
50
Many reports have indicated the presence of γ H2AX foci in non-irradiated cells.
For instance, we showed that about 1.5% of confluent human fibroblasts have 1 to 4 large
 γ H2AX foci per cell, with an average size of $1.7 \mu\text{m}^2$ that would appear to encompass
about 15 Mbp of DNA (10). Similarly, 6.3% of normal G0 human diploid cells have
phosphorylated ATM (ATMP) foci with diameters larger than $1.6 \mu\text{m}$ (i.e. $\sim 2 \mu\text{m}^2$) (11).
Others studies have noted large γ H2AX foci in senescent human cells and aged mice
tissues, and interpreted these foci to be due to unrepairable DSB (12). Generally, large
foci seen spontaneously or in senescent cells have imaging characteristics similar to
persistent radiation-induced foci. We will discuss later how these large foci may all
reflect similar chromatin status with different cellular outcomes.51
52
53
54
55
56
57
58
59
50
Fig. 1 shows typical images of γ H2AX/53BP1 dual staining of cycling non-
irradiated normal human mammary epithelial cells (i.e. MCF10A). As also observed in
fibroblasts (10), a population of growing epithelial cells typically shows a very mixed
 γ H2AX/53BP1 staining pattern. Even though many cells do not appear to contain foci, a
significant number of cells also show spontaneous foci. Some of this variability has
recently been associated to inter-individual factors (13) where quiescent G0/G1 normal
human fibroblasts were shown to have on average 0.2 to 2.6 γ H2AX foci/cell looking at
25 different normal human donors (overall mean \pm SD was 1.00 ± 0.57). Another

important aspect of γ H2AX immunostaining is illustrated in Fig. 1, where the existence of many small and low intensity foci in non-irradiated G1 cells is revealed by digitally enhancing the image. The imaging characteristics of these dim foci have been well described (14, 15), and their exhibited pattern is similar to S-phase cells. Although researchers have noted these foci in unexposed cells, similar types of foci have also been detected following IR. The function of these spontaneous or non-DSB related foci is still uncertain (14). In contrast, 53BP1 shows a uniform staining in the nucleus from G1 to G2, with exclusion in the nucleolus as illustrated in Fig. 1. On the other hand, as for γ H2AX, 53BP1 also shows spontaneous bright foci. γ H2AX foci typically colocalize with 53BP1 foci, the reverse is not always true as illustrated in the first upper panels of Fig. 1.

Using the fact that PCNA is bright in S-phase cells (16), we previously showed how S-phase cells typically have a diffuse and high background intensity with discrete punctate small γ H2AX foci (10). MCF10A nuclei with such imaging characteristics were visually selected and are displayed in Fig. 1. γ H2AX foci may be an indication of stalled or broken replication forks in S-phase (17). It was in fact hypothesized in a recent review (18) that ATRIP could phosphorylate H2AX at stalled replication forks, since ATRIP recognizes single-stranded regions in the DNA similar to regions during S-phase. Thus ATR mediated γ H2AX could lead to foci which do not necessarily mark DSB. Flow cytometry studies confirmed immunofluorescence results by showing that the intensity of γ H2AX staining increases as a cell moves through the cell cycle with cells in S/G2/M phases having a much larger fluorescence than the expected ~2 fold increase from G1 levels (17, 19). In contrast, no distinct pattern is typically observed for 53BP1 in S-phase (see Fig. 1).

Cells in metaphase contain γ H2AX foci that are ATM-dependent and may reflect a conserved mitotic function for this modification (15). Fig. 1 illustrates the very strong uniform signal of γ H2AX in mitosis, which seems maximum in metaphase and starts reducing in telophase. Similar observations have been previously published *in vivo* on mice germ cell mitotic chromosomes (20). In contrast, a complete loss of 53BP1 immunoreactivity is noted in the nucleus during mitosis, suggesting diffusion of 53BP1 into the cytoplasm.

To conclude this section, cell-cycle and inter-individuality are factors affecting the presence of spontaneous foci. The general consensus in the literature links these foci to unrepairable DNA damage, transient DSB or genomic instability. However one could challenge this “DNA-centric” view, as it has been shown that the binding of various repair factors to chromatin is sufficient to trigger foci formation in an ATM- and DNAPK-dependent manner in the absence of DNA damage (21).

RIF: imaging characteristics of early response to low-LET radiation

Numerous studies have detailed the appearance of RIF containing various proteins following exposure to different radiation qualities and quantified the induced foci microscopically by eye or with computational analysis. The first approach limits the analysis to small numbers of cells, limits the amount of information one can extract from the images, such as foci shape, size or intensity, and is prone to observer bias. Thus, in Table I we only summarize computer analysis of RIF reported within an hour following exposure to low-LET IR. Note that “normal cells” here means that these cells are not

5
6
7
8
9
10
11
12
13
14
15
16
17
18
19
20
21
22
23
24
neoplastic and does not necessarily mean they are primary cell lines. One result that can
25 be concluded from Table 1 is that even though DSB are generated immediately upon
26 exposure to radiation, not all RIF appear immediately. RIF frequencies reach a maximum
27 of ~10-40 RIF/nucleus/Gy approximately 15-30 min after exposure to low-LET. Similar
28 delays were shown using biochemical assays such as two-dimensional gel analysis,
29 reaching half-maximal value at 1 min and maximal value at 9–30 min post exposure (6)
30 or reaching maximum intensity at 15 to 30 min using flow cytometry (22). In contrast,
31 delays in DSB induction are not observed using pulse field gel electrophoresis – PFGE,
32 the standard method for detection of DSB. PFGE data show initial values of 25-35
33 DSB/Gy, with breaks immediately decreasing exponentially following IR (23, 24).
34 Illustration of such disparity is shown in Fig. 2A. There are many explanations for the
35 weak RIF detection prior to 30 min which are not mutually exclusive: 1. some DSB are
36 repaired by mechanisms that do not require foci formation; 2. some RIF remain below
37 detectable levels of phosphorylation; 3. some extra time is required to assemble enough
38 molecules at some sites before they become detectable (i.e. if the site is originally less
39 accessible).

25
26
27
28
Table 1: Characteristics RIF frequencies and sizes for low-LET induced foci

29 30 31 32 33 34 35 36 37 38 39 40 41 42 43 44 45 46 47 48 49 50 51 52 53 54 55 56 57 58 59 60 61 62 63 64 65 “NORMAL” HUMAN	Species	Marker	Cell	Dose (Gy)	T _{max} (min)	Max (RIF/Gy)	Foci size (μm ²)	Ref
	Breast epithelial	γH2AX	HMEC 184	1	30	15.9	0.35 @ 30 min	(25) (Table I)
	Skin fibroblast	γH2AX	HCA2	0.1-3	45-120	13	0.2-0.35 (5 min - 1 hr)	(10) (Fig. 3A,B)
	Fibroblast	γH2AX	HF19	1	20-30	19.1	--	(26) (Fig. 3)
	Fibroblast	γH2AX	25 lines	0.05-0.25	10-30	14-21	--	(13)
	Breast epithelial	ATMp [*]	HMEC 184	1	30	16.0	0.35 @ 30 min	(25) (Table I)
	Skin fibroblast	ATMp [*]	HCA2	0.1-3	30	35	0.14 (5 min – 2 hr)	(10) (Fig. 5A,B)
	Diploid fibroblast	ATMp [*]	HE49	0.1-1	15	36.9	~0.28@1 hr (Ø~0.6μm)	(11) (Fig. 1A,C)
	Breast epithelial	53BP1	HMEC 184	1	30	16.3	0.35 @ 30 min	(25) (Table I)
HUMAN TUMOR	Diploid fibroblast	53BP1	HE49	0.1-1	15	~37	~0.28@1 hr (Ø~0.6μm)	(11) (Fig. 4A,C)
	Melanoma	γH2AX	HT144	2	30-60*	22	0.1-0.12	(22) (Fig. 3)
	Cervical	γH2AX	SiHa	2	30-60*	16	0.1-0.12	(22) (Fig. 3)

	Osteosarcoma	53BP1	U2OS	0.5-8	30	23	--	(3) (Fig. 4B,D)
“NORMAL” HAMSTER	Ovary	γH2AX	CHO	0. 1-1	20	20	--	(27) (Fig. 2)
	Lung	γH2AX	V79-4,	1	20-30	12.2	0.2	(26) (Fig. 1,3)
	Lung	γH2AX	V79	2	30*	25or 10	0.1-0.12	(22) (Fig. 2)

+ ATMp: phosphorylated (pS1981) ATM

* Information provided in text, not shown in Fig.s.

Foci frequencies have been shown to be proportional to the amount of dose delivered to a cell in the low dose range. One study originally reported a constant value of 35 RIF/Gy three minutes following IR using doses ranging from 1.2 mGy to 2 Gy (28). There are however many confounding factors for accurate RIF quantification. First, γH2AX is known to occur as a normal process during the cell cycle as discussed previously. For example, IR induces higher levels of γH2AX in S-phase cells as measured by microscopy (10) but there is less induction per Gy in S-phase cells as compared to G1 cells as shown by flow cytometry (17). Second, the sensitivity of the optics used to acquire images and the type of algorithms used to detect a focus or the criteria used to score a RIF by eye can lead to additional discrepancies between labs. Finally, statistical significance is hard to achieve at low doses. For example, in the study previously mentioned, ~16 to 32 RIFs were scored by eye in a total of 400 to 800 primary human lung MRC-5 fibroblasts when exposed to 1.2 mGy, leading to $16/400/1.2e-3 = 33.3$ RIF/cell/Gy. One might ask how such a low number of scored RIF is enough to get statistical significance. One argument the authors give in their ability to resolve RIF at such a low dose is the fact the cells they used had a very low level of spontaneous foci (i.e. ~0.05 spontaneous foci/cell against ~0.04 RIF/cell at 1.2 mGy). One recent study circumvented the foci background issue by looking at live cells where one knows exactly how many foci there is before IR allowing identification of real RIF after exposure to IR. In this study (29), the authors also showed a linear response following 5 mGy to 1Gy of low-LET radiation in the human epithelial fibrosarcoma cell line HT1080 stably transfected with 53BP1YFP 30 min post-IR. Note however that even though this study reported linearity, very different levels of damage were observed depending on the cell line used: i.e. 16-20 RIF/Gy for both γH2AX and 53BP1-YFP in HT1080 versus 60 RIF/Gy for a hTERT immortalized normal human bronchial epithelial line (HBECs) that stably express (EGFP)-tagged-53BP1. RIF numbers were determined using the same microscope, the same quantification, and the same optics, again highlighting the importance of cell type in the number of RIF. Such discrepancies clearly weaken the usage of RIF as a pure indicator of DNA DSB, as physics predicts similar numbers of DSB for the same dose and genome size.

In the high dose range, departure from linearity has been observed. For example, we showed γH2AX RIF yields are 30 to 40% lower between 1 and 3 Gy than below 1 Gy, 1 hr post-IR in normal human fibroblast (10). Lower RIF yields per Gy at doses larger than 1 Gy may be due in part to a resolution problem, as with higher doses there is more potential for overlapping foci. However we and others have also shown that smaller γH2AX foci are produced following doses greater than 0.5 Gy in the first hour post-

5
6
7
8
9
10
11
12
13
14
15
16
17
18
19
20
21
22
irradiation, which should reduce foci overlapping at higher doses (10, 22). In addition, it
23
24
25
26
27
28
29
30
31
32
33
34
35
36
37
38
39
40
41
42
43
44
45
46
47
48
49
50
51
52
53
54
55
56
57
58
59
60
was recently shown at low doses, were foci overlap was unlikely, that RIF yield
decreased consistently between 5 cGy and 25 cGy, with averages over 18 different
normal human fibroblasts going from 21 RIF/Gy to 17 RIF/Gy respectively (13). These
changes are evidently small and difficult to quantify statistically at low dose. However,
other methods that do not need to resolve foci such as measuring the total γ H2AX
intensity per cell or using flow cytometry also suggest saturation at higher doses (22). In
reviewing the data, it is noteworthy that dose response slopes are 2 to 3 times higher
between 0 and 1 Gy than between 1 and 8 Gy for various human and hamster cell lines
(22). In contrast, other studies have looked at 10 different cell lines suggesting linearity
for the total intensity of γ H2AX from 1 to 4 Gy, with the exception of the human breast
line MCF7 and the HT1080 line showing lower relative immunofluorescence at 3 and 4
Gy (30). In this later study however, it is hard to conclude there was no saturation for the
8 other cell lines as no measurements below 1 Gy were available making it impossible to
estimate the initial slope in the low dose range.

23
24
25
26
27
28
29
30
31
32
33
34
35
36
37
38
39
40
41
42
43
44
45
46
47
48
49
50
51
52
53
54
55
56
57
58
59
60
Overall, the literature cited here suggests a loss of detection with increasing dose,
with clear saturation taking place in general above 1 Gy. As for spontaneous foci, large
inter-individual variations were noted in this phenotype as well. Lower yield at higher
dose most likely reflects saturation at the kinase level (e.g. lower foci size for higher dose
suggests this) and it would be interesting to see if the level of p53 in different cells
correlate with sensitivity to saturation, as p53 has been suggested to play a role in
modulating the levels of γ H2AX in different cells (31). Another potential explanation of
saturation is the limited amount of substrate. This is at least possible for H2AX, where a
recent study using high resolution 4Pi microscopy (32) showed that H2AX was randomly
distributed into ~5000 separate nuclear clusters (i.e. HeLa cells).

36 **DNA damage sensing as a function of radiation quality**

37
38
39
40
41
42
43
44
45
46
47
48
49
50
51
52
53
54
55
56
57
58
59
60
High-LET particles deposit energy along their trajectory and therefore present
interesting opportunities for studying the spatial organization of RIF. Another distinction
between high and low-LET is in the complexity of the generated DSB. For the following
discussion we will designate a DSB with one (or more) break(s) within 10 bp as simple
DSB, and a DSB with two or more breaks on each strand within 10 bp as complex DSB.
As LET increases, 30% of DSB are simple DSB and 70% are complex DSB (33, 34). In
contrast, only 30% of the DSB induced by low-LET are complex DSB. When monolayer
of cells are exposed perpendicular to a high-LET particle beam, each impact induces
many complex DSB within a very restricted area and RIF frequencies reflect particle
fluence instead of individual DSB (10, 26, 35). As illustrated in Fig. 2D, it is difficult to
resolve individual foci within the tracks produced when cells are irradiated in this manner
due to the much poorer resolution of a microscope along the Z-axis. We have previously
shown that RIF formation is faster following exposure to high-LET N ions (132 keV/um),
with a maximum number of foci detected 10-15 min post-IR instead of 30-45 min for
low-LET in normal human fibroblasts (10). In addition, high-LET RIF typically detect
100% of the tracks as shown by us and others (10, 35) and their size increases twice as
fast as for low-LET, resulting in a three-fold increase during a 2 hour period (10). Since
high-LET particles induce more complex DSB, these data suggest that severe lesions
seem to induce a faster and more robust RIF formation.

5
6
7
8
9
10
11
12
13
14
15
16
17
18
19
20
21
22
23
24
25
26
27
28
29
30
31
32
33
34
35
36
37
38
39
40
41
42
43
44
45
46
47
48
49
50
51
52
53
54
55
56
57
58
59
60
61
62
63
64
65
On the other hand, the speed at which RIF are resolved remains unclear at this point as there are contradicting reports. In normal human fibroblast, we showed that foci frequency remain high up to two hours following N ions (150 keV/μm), whereas other investigators showed using computer-based analysis in Chinese hamster cells V79-4 fast foci loss matching PFGE DSB rates after exposure to alpha particles (3.31 MeV, 120 keV/μm at such energy) (26). However, one could argue that the kinetic response in hamsters is different and perhaps faster. In addition, perpendicular beam orientation complicates interpretation of the response as the amount of DSB per focus will vary greatly with the shape of the cells, the LET, the atomic number, and the energy of the particle. Differences in foci frequency or kinetics could also be attributed to physical differences in the radiation quality. To circumvent this problem and better resolve damage along high-LET tracks, cells can be irradiated with high-LET particle beams parallel to cell layer (25, 36, 37). As illustrated in Fig. 2E, since the XY resolution of a microscope is much higher than the Z, and cells grown as monolayer are elongated in the XY plane, foci can be differentiated more easily when irradiation is performed this way. Using such configuration we could show that γH2AX and 53BP1 RIF following high-LET exposure (i.e. 150 keV/μm, Fe ions) in human epithelial cells were maximum as early as 5 min post-IR with maximum frequencies ~ 0.7-0.9 RIF/μm along Fe ion tracks (25). In addition, RIF resolution had a 4 to 6 hours half life which is slower than PFGE measurements, with a reported 2 hour half life in human glioma exposed to 10 Gy of 125 keV/μm N ions (38) or a 3 hour half life in normal human fibroblast cells in G1 after 80 Gy of 150 keV/μm Fe ions (39). This difference of kinetic is illustrated further in Fig. 2C assuming for illustration purposes a 2.5 hour half-life for the theoretical DSB kinetic. Interestingly, increasing LET does not seem to change the number of RIF along a track as other studies reported ~0.5-1 γH2AX RIF/μm along Carbon ions of 200 keV/μm or 0.96 XRCC1 RIF/μm for Uranium ions of 14,300 keV/μm (40). Theoretical computations for these high-LET horizontal tracks predicted the number of DSBs/μm to be 1.1, 2.6 and 187 for Fe, C and U respectively IR (25, 40). Thus, as energy deposition along track increases with LET, the number of foci remains the same but more DSBs must be comprised in each one of them, suggesting a mechanism for the high dose saturation previously mentioned for low LET. The slower foci resolution for high-LET may then simply reflect the fact that multiple DSBs are within each focus and thus it takes longer to repair all DSB within one focus.

46 47 DNA damage response is modulated by chromatin density

48
49
50
51
52
53
54
55
56
57
58
59
60
61
62
63
64
65
Evidence from recent years suggests that chromatin organization mediates the response to DNA damage. The mechanism by which this happens remains unclear, but local chromatin structure appears to play a role. Chromatin decondensation around the DSB is believed to be an important trigger for ATM dimer dissociation and subsequent ATM autophosphorylation and activation (7, 41). Similarly, DSB induce a local higher-order chromatin changes unmasking methylated lysine 79 on histone H3, which serves as the binding site for 53BP1, a critical DNA repair protein (42). The phosphorylation of histone H2AX by ATM, ATR and DNA PKcs near the DSB is also a chromatin modification critical to the repair process (6, 43). γH2AX has been proposed to play a major role in chromatin remodeling itself by promoting biochemical interactions between multiple proteins following exposure to radiation (44). The rapid outward spread of this

5
6
histone modification from the site of the DSB has recently been suggested to be a key
event in homologous recombination during G2 phase (45).

7
8
9
10
11
12
13
14
15
16
17
18
19
10 In our recent study on 1 GeV/amu Fe track induced damage (25), we noted that
11 γ H2AX, pATM and 53BP1 RIF distribution along a track was not random, and was
12 characterized by a regular spacing of 1.2 μ m between consecutive RIF instead of the
13 more likely 0.5 μ m spacing predicted by theoretical modeling. Optical properties of the
14 microscope and physical characteristics of Fe ion energy deposition were all taken into
15 account in this theoretical computation. It is noteworthy that the deviation from
16 randomness was significant at the time points measured, 5 to 30 min post-IR. In addition,
17 simulations also predicted that DSB should be more likely in regions with more DNA
18 (i.e. heterochromatic regions) whereas our experimental results actually showed more
19 RIF in low-DAPI regions (i.e. euchromatin) or at the euchromatin/heterochromatin
20 interfaces. A recent study further confirmed this finding by co-staining with specific
21 markers such as non-histone chromatin protein HP1 and trimethylated-H3K9 (46). The
22 authors concluded that DSB-inducing agents failed to efficiently generate γ H2AX foci in
23 heterochromatin, perhaps due to the epigenetic or packaging properties of the
24 heterochromatin. Similarly, other investigators have shown that detection of γ H2AX
25 using CHIP assays was significantly lower on heterochromatic satellite 2 sequences and
26 α -satellite repeats (47).

27
28
29 There are many possible reasons explaining the observed RIF spatial distribution
30 with respect to chromatin density. For example, reactive oxygen species generated by IR
31 may be more efficiently scavenged by the higher concentration of histone in the
32 heterochromatin than in the euchromatin. This would lead to the observed lower number
33 of RIF in the heterochromatin (25, 46, 47). Supporting this idea, hypotonic treatments,
34 which lead to the swelling of the nucleus and thus poorer radical scavenging, can induce
35 a 3 to 5-fold increase in DSB yield (48, 49). Similarly, histone deacetylase (HDAC)
36 inhibitors have gained considerable interest recently in enhancing anti-cancer therapy by
37 increasing the acetylation of core histones, resulting in an open chromatin configuration
38 that is more accessible to DNA-targeting agents. When HDAC inhibitors were used in
39 conjunction with radiation, more γ H2AX RIF were induced, they often decayed slower
40 and tumor cells were sensitized to radiation (50-53). Of course, one could also interpret
41 these results as HDAC participating in the repair directly and not necessarily participating
42 in chromatin relaxation.

43
44
45 The observed RIF spatial distribution may also reveal important distinctions in the
46 way DSB are detected in different chromatin regions. One could hypothesize that only a
47 complex DSB in the heterochromatin leads to a RIF and its formation would require the
48 DSB to first move close enough to the euchromatin. In contrast, any DSB generated in
49 the euchromatin would lead to a rapid induction and resolution of RIF. This would
50 explain why more RIF are generally observed in the euchromatin. Thus, when inducing
51 only simple DSBs one would expect to see fast foci induction. Accordingly, Soutoglou
52 and Misteli observed a fast kinetic of foci formation where breaks were induced by I-SceI
53 endonuclease (54). In contrast, foci induction would be much slower in the
54 heterochromatin due to the time it takes to move DSB to the interface, and RIF resolution
55 would be much slower due to the complexity of these damages. Such a concept is
56 illustrated in Fig. 3 and indicates the contribution of each type of DSB and chromatin
57 territory in the observed RIF kinetic. In support of this model, recent studies suggest that
58
59
60
61
62
63
64
65

5 heterochromatic RIF resolve slowly and that their resolution is ATM-dependent. In
6 addition, observations (55, 56) and image quantifications (25) revealed that γ H2AX RIF
7 appear preferentially at the periphery of heterochromatic domains rather than within these
8 domains. Physics tells us that preferential location of damage at these interfaces cannot
9 be due to specific deposition of radiation within the nucleus (25), and instead suggests
10 that damages in the heterochromatin may need to be moved towards the euchromatin to
11 be detected and processed. Although the hypothesis of foci movement to the periphery of
12 the heterochromatic domain is highly speculative, and we cannot exclude that other
13 mechanisms prevent the formation of foci in heterochromatin, a relocalization of
14 heterochromatic regions to the periphery of the domain has been previously described for
15 explaining the conformation of heterochromatin during replication (57). Moreover,
16 movement of large segments of DNA is not a new concept: it has been shown that some
17 genes become transcriptionally active only upon relocating into open regions of the
18 nucleus (58). In fact, whole parts of chromosomes have been reported to move over a 1 to
19 5 μ m distance within a few minutes post transcription activation in mammalian cells (59).
20 Such movements are hypothetically illustrated in Fig. 3B with arrows indicating the DSB
21 movement from the original position within the heterochromatin (DAPI bright region in
22 the image) to the chromatin interface where detection could take place.
23
24

25 If the relocalization of heterochromatic DSBs to the periphery of the compact
26 domain turns out to be true, it would be extremely important to establish which
27 mechanism is responsible for this movement. Is it possible, for example, that some
28 sensors of the damage are able to detect it and actively promote its movement at the
29 periphery of the heterochromatic region, despite the compaction of heterochromatin?
30 Would that imply that the involved repair pathways are different in the euchromatin and
31 the heterochromatin? It is also possible that heterochromatin relaxation, occurring in the
32 presence of DSBs, allows the increasing mobility of heterochromatic DNA thus
33 facilitating the stochastic movement of DSBs to a more peripheric area, where they are
34 ultimately detected. Some data suggest that at least some of the DSB sensors are indeed
35 able to access heterochromatin for detecting the lesions. For example, in human cells, the
36 induction of DSBs with laser directed toward the heterochromatic domain results in local
37 HP1b phosphorylation by the casein kinase within 5 min, suggesting that this kinase can
38 access the compact heterochromatic domain (60). Similarly, the evidence that ATM-
39 phosphorylates Kap1 six min post-IR, which is important for promoting heterochromatin
40 relaxation, implies that the original break in heterochromatin is able to trigger local ATM
41 activity before the relaxation occurs (55, 56).

42 It is interesting to note that recent reports showed that HP1, which is known to
43 play a role in stabilizing heterochromatin compaction, is also recruited to laser-induced
44 DSBs. This might suggest the importance of rendering the DSB site less 'movable' for
45 facilitating accurate repair (61, 62). In this view, the more rigid structure of
46 heterochromatin might intrinsically protect it from inaccurate repair by stably tethering
47 DNA ends allowing them to stay in place. Such an idea has been supported by reports
48 showing that chromosomal aberrations occur preferentially in the euchromatin and not in
49 the heterochromatin (63). Bailey and Bedford recently reviewed this topic and
50 summarized a number of studies where radiation-induced translocations were less
51 frequent in the condensed inactive X-chromosome than in its active counterpart (64).
52
53
54
55
56
57
58
59
60
61
62
63
64
65

Persistent RIF: unrepaired DSB, mis-repaired DNA and/or permanent chromatin modification?

DSB repair measured by electrophoresis or neutral filter-elution (23) has a rapid component (5-30 min half-life) and a slower component likely related to the resolution of complex DSB (4 to 10 hours half-life). Taking into account that ~30% of low-LET radiation DSB are complex DSB (33, 34), one would therefore predict that out of the 25 DSB/Gy generated by low-LET (24) about 17 DSB/Gy would be repaired by fast kinetics, and 8 DSB/Gy by a slower kinetics. Thus at 24 hrs post-IR, we would expect to have at most 1 DSB/Gy still undergoing repair. Although this single or small number of RIF would be hard to be accurately measured because of spontaneous foci within a cell, several studies have observed persistent foci days following low-LET exposures. For example, normal human fibroblasts irradiated with low-LET showed persistent foci for 5 days following 4 Gy of X-rays even though by that time all DSB should be fully resolved (65). These persistent γ H2AX RIF were large and co-localized with ATMp as well as with p53 phosphorylated at serine 15, suggesting ongoing processing. Rather than concluding that RIF represented un-repaired DSB, these authors concluded that persistent foci were revealing a chromatin alteration, which resulted in the induction of a senescence-like growth arrest following IR. Senescence-like growth arrest is a p53-dependent irreversible G1 arrest thought to suppress radiation-induced telomere dysfunction following genomic instability in fibroblasts. This same group also showed that persistent RIF were detected on intact metaphase chromosomes that did not contain any chromosome fragments 96 hours following low-LET exposure, suggesting again that these foci may indicate an aberrant chromatin structure due to illegitimate rejoining (66). More recently they extended their work to show that the large foci have a role in triggering G1 arrest: the larger the foci, the brighter the p53 phosphorylation, the more likely cells would arrest (11).

Other studies looking at earlier time points (2 to 12 hours) also showed that γ H2AX RIF could still be observed even at time points when other methods of DSB quantification, such as chromatid breaks staining with Giemsa in metaphase or PFGE suggest that repair is completed (20, 67). Even though one might consider such results as a proof of the much greater sensitivity of RIF for detecting DSB, this may also indicate that persistent RIF may not necessarily mark DSB. Similarly, mitotic nuclei exposed to IR have a slower rate of γ H2AX foci loss than DSB loss as measured by PFGE (27), likely due to the fact the heterochromatic RIF take longer to resolve (55). Therefore large persistent foci may be the result of damages occurring in denser regions of the chromatin leading to permanent structural changes.

Fig. 4 summarizes the possible fate of cells within the first 48 hours post-IR. As previously discussed, the most likely outcome for a fibroblast with persistent foci would be growth arrest. Growth arrest might also be the most likely outcome when RIF are marking sites of permanent DNA damage. On the other hand, when DNA has been fully repaired but the repair process has led to permanent changes in the chromatin structure, leading to persistent RIF, there seems to be no reason for the cell to stop dividing. In fact, RIF have been shown to be replicated in daughter cells (68) and chromatin architecture is known to be highly conserved. For example, it was shown in CHO cells stably expressing GFP-histone H2B, that GFP photobleaching patterns could be

5 replicated in daughter cells, suggesting histones were equally segregated at the same
6 nuclear positions in each daughter cell during mitosis (16). In this study, the authors
7 concluded that duplication of chromatin pattern might be an epigenetic mechanism to
8 maintain cell differentiation. Therefore, if we assume large persistent RIF are marking
9 altered organization of the chromatin, these marks may also relate in some instances to a
10 persistent altered epigenetic programs leading to heritable altered phenotypes.

11 In summary, euchromatin damages are repaired faster but may lead to more
12 chromosomal rearrangements, whereas, damages in the heterochromatin may be more
13 accurately repaired but may lead to irreversible chromatin structural changes. We assume
14 here that the more condensed the chromatin is, the more reorganization it will undergo
15 during repair, and the more likely permanent changes of chromatin structure will be
16 observed. Indeed, the slower RIF kinetic in mitotic DNA or heterochromatic regions
17 previously discussed suggest that chromatin modifications are more difficult to occur in
18 dense regions of the DNA. In addition, reported sizes of RIF in mammalian cells has led
19 to estimation of 1 to 4 Mbp of DNA by gel electrophoresis at early times post exposure
20 (6), with maximum sizes of 15-30 Mbp reached two hour post-IR (10, 18, 69, 70). We
21 may then wonder what is more deleterious: the loss of a few kbp of DNA, or epigenetic
22 alterations over tens of Mbp? In the former case, mis-repaired DNA rarely leads to
23 deleterious effects (e.g. $\sim 10^{-5}$ to 10^{-6} mutations/cell/Gy for HPRT locus (71)), whereas
24 changes of chromatin architecture over Mbp will definitely have an impact on the
25 transcriptome of a cell.

26 Thinking of chromatin as a target of ionizing radiation and permanent chromatin
27 alterations as a mark detectable by persistent RIF opens the door to an unexplored
28 mechanism for radiation-induced phenotypes. For example, epigenetic changes marked
29 by persistent RIF could be another factor influencing radiation-induced genomic
30 instability. As reviewed by various investigators (72, 73), a mis-repaired DSB is typically
31 considered to be an important potential inducer of genomic instability. However a large
32 study on the panel of NCI-60 tumor cells correlated chromosomal rearrangement with
33 γ H2AX foci frequency and concluded that chromatin instability might be responsible in
34 part for higher foci frequency (74). In addition, the relationship between mutations (i.e. a
35 measure of mis-repaired DSB) and genomic instability is difficult to reconcile: i.e. there
36 is a large discrepancy between the very small rate of DNA mutation induced by low-LET
37 and the high yield of radiation-induced genomically unstable cells (1 to 30%) (72). If
38 DNA mutations were the cause of genomic instability, one should observe much lower
39 frequencies of genomic instability. On the other hand, with a reported persistent RIF
40 frequency between 30 to 40%, 24 to 120 hours following low -LET exposure in normal
41 fibroblasts (65, 66), persistent changes in chromatin marked by RIF match more closely
42 the rates of genomic instability. This is an interesting speculation that should be further
43 investigated.

52 53 Conclusion

54 The assumption that RIF only reflect the presence of a DSB has caused a number
55 of misconceptions in the field of radiation biology, as scientists often refer to them as a
56 DSB when in fact they are only marks of chromatin modifications. It is our hope that we
57 have provided evidence to indicate that damages other than DSB, such as architectural
58 changes in the chromatin can result in RIF. This manuscript emphasized the importance
59
60
61
62
63
64
65

5
6
7
8
9
of not equating RIF with DSB in all situations and showed how dose and time
dependence of RIF frequency is inconsistent with a one to one equivalence.

10
11
12
13
14
15
16
17
18
19
1
As summarized in Fig. 4, we tried to reconcile data from the literature by adding
chromatin as a main factor in the foci response. Briefly, upon irradiation, DSB are
generated and cause immediate chromatin decondensation in euchromatin and rapid
formation of RIF. In heterochromatin, the packaging of DNA moderates this response
and only complex breaks elicit RIF which have slower formation and resolution. In
addition, for doses larger than 1 Gy, or after exposure to high-LET, RIF most likely
reflect clusters of multiple DSBs and RIF remain longer in the nucleus. If repair has
failed or has led to chromatin alterations that cannot be restored, the mechanical forces
signaling DNA sensing proteins remain active leading to persistent RIF. Persistent RIF
or large foci seen spontaneously in non-irradiated cell lines may reflect regions where
chromatin architecture is damaged or is undergoing remodeling. In fibroblasts, such
alterations have been linked to permanent growth arrest. On the other hand, one could
hypothesize that if DNA has been repaired but chromatin organization could not be
restored, a cell would resume its cell cycle allowing replication of RIF. Therefore,
heritable persistent RIF spanning over tens of Mbp may affect the transcriptome of a
large progeny of cells leading to the emergence of new and stable phenotypes. Such
model opens the door to a “non-DNA-centric view” of radiation-induced phenotypes.

2
3
4
5
6
7
8
9
10
11
12
13
14
15
16
17
18
19
20
21
22
23
24
25
26
27
28
29
30
31
32
33
34
35
36
37
38
39
40
41
42
43
44
45
46
47
48
49
50
51
52
53
54
55
56
57
58
59
60
61
62
63
64
65

ACKNOWLEDGEMENTS

We apologize to all authors whose publications have not been cited due to space limitation and conciseness of the manuscript. We would like to thank Dr. G. Karpen, Dr. P. Olive, Dr. B. Rydberg and Dr. T. Groesser for their useful comments on the manuscript and their engaging scientific discussions. We also thank the National Aeronautics and Space Administration, which sponsors our research on RIF under grant no. T6275W, NASA Specialized Center for Research in Radiation Health Effects.

This work was supported by the U.S. Department of Energy under Contract No. DE-AC02-05CH11231.

7
8
9
10
11
12
13
14
15
16
17
18
19
20
21
22
23
24
25
26
27
28
29
30
31
32
33
34
Figure legends:

35
36
37
38
39
40
41
42
43
44
45
46
47
48
49
50
51
52
53
54
55
56
57
58
59
60
61
62
63
64
65
Fig. 1: Example of typical γ H2AX/53BP1 dual staining in cycling normal non-irradiated human mammary epithelial cells (MCF10A). In these images, as previously described (25), γ H2AX has been fluorescently labeled in red with mouse monoclonal anti phospho-histone H2AX (Ser139) antibody (1.42 μ g/ml; Lot # 27505; Upstate Cell Signaling Solutions Inc. Charlottesville, VA) and secondary Alexa 594 (at 1:300 from Molecular Probes, Invitrogen, Carlsbad, CA). 53BP1 has been fluorescently labeled in green with rabbit polyclonal anti 53BP1 (5 μ g/ml, lot # A300-272A, Bethyl Lab, Montgomery, TX) and secondary Alexa 488 (at 1:300 from Molecular Probes, Invitrogen, Carlsbad, CA). Cells have been counter stained with DAPI label nuclear DNA (blue). Each channel represents one center slice of a cell acquired with the same exposure time and digital camera gain. Each row depicts a different phase of MCF10A, going from G1 (top) to mitosis (bottom). G1 cells typically show no γ H2AX foci or few bright γ H2AX foci. However, if the γ H2AX channel gained is increase by a factor 3, the presence of many dim foci is then visible (upper right panel). In contrast, 53BP1 shows a pattern in G1 that typically matches DAPI signal, with some spontaneous foci as well. DAPI and 53BP1 pattern similarity disappears during S-phase, even though 53BP1 signal remains uniform and elevated. γ H2AX immunoreactivity is significantly increased during S-phase with pattern similar to the dim foci revealed by gained enhancement in G1. As cells move to mitosis, γ H2AX immunoreactivity further increases as depicted with a fully saturated signal in metaphase that needs to be acquired with half the gain in order to not saturate the image. γ H2AX pattern in mitosis matches DAPI, revealing full phosphorylation of this histone in the condensed chromosomes. In contrast, 53BP1 seems to be progressively excluded from the nucleus during mitosis.

36
37
38
39
40
41
42
43
44
45
46
47
48
49
50
51
52
53
54
55
56
57
58
59
60
61
62
63
64
65
Fig. 2: Hypothesized foci frequency curves for different radiation qualities and exposure regimens. Upper panels (A,C) depict relative RIF frequencies which would be expected with each radiation quality and compared to the expected relative DSB kinetic as measured by PFGE; lower panels (B,D,E) depict geometrical configuration of cells grown as monolayer during irradiation, with dotted lines representing direction of high-LET beam across cells (D and E); the XY plane depicts the way RIF will be visualized microscopically, with representative RIF sizes. (A,B) schematize the low-LET RIF kinetics, where geometrical configuration has no effect. Both percentages of RIF (solid line) and DSB (dotted line) per nucleus with respect to the initial expected number of DSB (DSB(0)) are graphed with the curves reflecting the lack of foci detection for DSB repaired within the first 30 min. Kinetic curves are based on the assumption of a 30 min half life for DSB repair after low-LET and show good correlation with DSB kinetic after 30 min (symbolized by $RIF \propto DSB$). (C) schematizes the relative RIF frequency normalized to its maximum value following high-LET exposure. Normalizing to the expected number of DSB is not done here as RIF for high-LET reflects more DSB clustering. High-LET typically induces a slower DSB repair and is approximated here with a 2.5 hours half-life for LET \sim 150 keV/ μ m (38, 39). In contrast, high-LET RIF have been shown to have an even slower resolution half-life of 5 hours (25). Two possible geometries can be applied for high-LET, with a beam perpendicular to the plate (D),

leading to multiple DSB in a single focus per track when visualizing foci or with beam parallel to the plate (E). In the perpendicular configuration, foci frequencies correlate with track traversal (symbolized by *RIF* \propto *Tracks*), not DSB. The horizontal configuration (E) leads to visual track with multiple larger foci along it. Such geometry permits evaluation of the number of RIF/ μ m along the track instead of the classic RIF/nucleus. The slower kinetic for high-LET reflects repair of complex damages as well as clustering of these damages into single foci. One must note here that high energy particles (HZE) are more favorable for such a geometrical configuration, since particles must go through mm to cm of media and plastic. As has been previously described, for lower particle energies, one has to angle slides in such a manner as to allow the beam to hit the bottom of the slide to avoid traversal through large amounts of medium (40, 75).

Fig. 3: Hypothetical contribution of Simple and Complex DSB for the classic low-LET RIF kinetic. The left panel repeats the low-LET kinetic curves shown in Fig. 2A with an interpretation of the different types of DSB contributing to the RIF kinetics. The majority of DSB are immediately detected by RIF in the euchromatin (abbreviated Eu) whereas only complex DSB in heterochromatin (abbreviated Het) are detected by RIF and their detection is delayed due to the time it takes to move a DSB to the interface next to euchromatin DNA. The right panel illustrates the kinetic by showing a human cell stained for DAPI with hypothetical regions of DNA damage following IR. Simple DSB are noted as circles and complex DSBs as larger stars. At 0 min, initial damages are shown with blue DSB in low DAPI regions (euchromatin) and red DSB in bright DAPI regions (heterochromatin). At 5 min, only DSB in euchromatin have led to RIF (green full circles), whereas complex DSBs in the heterochromatin need to move towards DAPI dim regions as noted by red arrows before being detected at 30 min (shown as green full circles with red edges to note their origin from the heterochromatin). Permanent DNA or chromatin changes are marked by larger RIF sizes at 48 hours and are more likely to occur from complex DSB as depicted here.

Fig. 4: RIF formation/resolution and cell fate. Boxed legends indicate what type of damages foci mark. Bold text indicates corresponding chromatin status for each of these foci types. Small arrows in the flow chart indicate lower probability of events to take place based on discussion in the text. For example, cells with persistent RIF related to unrepaired DNA will most likely be eliminated (large arrow, cross). On the other hand, when a RIF marks chromatin changes where DNA damage was repaired successfully, there should be no obstacles for a cell to resume division (small arrow) allowing replication of its aberrant chromatin.

6
7
8
9
10
11
12
13
14
REFERENCES

15 1. T. Haaf, E. I. Golub, G. Reddy, C. M. Radding and D. C. Ward, Nuclear foci of
16 mammalian Rad51 recombination protein in somatic cells after DNA damage and its
17 localization in synaptonemal complexes. *Proc Natl Acad Sci U S A* **92**, 2298-2302
18 (1995).

19 2. T. Ashley, A. W. Plug, J. Xu, A. J. Solari, G. Reddy, E. I. Golub and D. C. Ward,
20 Dynamic changes in Rad51 distribution on chromatin during meiosis in male and female
21 vertebrates. *Chromosoma* **104**, 19-28 (1995).

22 3. L. B. Schultz, N. H. Chehab, A. Malikzay and T. D. Halazonetis, p53 binding
23 protein 1 (53BP1) is an early participant in the cellular response to DNA double-strand
24 breaks. *J Cell Biol* **151**, 1381-1390 (2000).

25 4. R. S. Maser, K. J. Monsen, B. E. Nelms and J. H. Petrini, hMre11 and hRad50
26 nuclear foci are induced during the normal cellular response to DNA double-strand
27 breaks. *Mol Cell Biol* **17**, 6087-6096 (1997).

28 5. B. E. Nelms, R. S. Maser, J. F. MacKay, M. G. Lagally and J. H. Petrini, In situ
29 visualization of DNA double-strand break repair in human fibroblasts. *Science* **280**, 590-
592 (1998).

30 6. E. P. Rogakou, D. R. Pilch, A. H. Orr, V. S. Ivanova and W. M. Bonner, DNA
31 double-stranded breaks induce histone H2AX phosphorylation on serine 139. *J Biol
32 Chem* **273**, 5858-5868 (1998).

33 7. C. J. Bakkenist and M. B. Kastan, DNA damage activates ATM through
34 intermolecular autophosphorylation and dimer dissociation. *Nature* **421**, 499-506 (2003).

35 8. D. W. Chan, B. P. Chen, S. Prithivirajsingh, A. Kurimasa, M. D. Story, J. Qin and
36 D. J. Chen, Autophosphorylation of the DNA-dependent protein kinase catalytic subunit
37 is required for rejoining of DNA double-strand breaks. *Genes Dev* **16**, 2333-2338 (2002).

38 9. B. P. Chen, D. W. Chan, J. Kobayashi, S. Burma, A. Asaithamby, K. Morotomi-
39 Yano, E. Botvinick, J. Qin and D. J. Chen, Cell cycle dependence of DNA-dependent
40 protein kinase phosphorylation in response to DNA double strand breaks. *J Biol Chem*
280, 14709-14715 (2005).

41 10. S. V. Costes, A. Boissiere, S. Ravani, R. Romano, B. Parvin and M. H. Barcellos-
42 Hoff, Imaging features that discriminate between foci induced by high- and low-LET
43 radiation in human fibroblasts. *Radiat Res* **165**, 505-515 (2006).

44 11. M. Yamauchi, Y. Oka, M. Yamamoto, K. Niimura, M. Uchida, S. Kodama, M.
45 Watanabe, I. Sekine, S. Yamashita and K. Suzuki, Growth of persistent foci of DNA
46 damage checkpoint factors is essential for amplification of G1 checkpoint signaling. *DNA
47 Repair (Amst)* **7**, 405-417 (2008).

48 12. O. A. Sedelnikova, I. Horikawa, D. B. Zimonjic, N. C. Popescu, W. M. Bonner
49 and J. C. Barrett, Senescent human cells and ageing mice accumulate DNA lesions with
50 unrepairable double-strand breaks. *Nat Cell Biol* **6**, 168-170 (2004).

51 13. P. F. Wilson, P. B. Nham, S. S. Urbin, J. M. Hinz, I. M. Jones and L. H.
52 Thompson, Inter-individual variation in DNA double-strand break repair in human
53 fibroblasts before and after exposure to low doses of ionizing radiation. *Mutat Res*
54 (2009).

55
56
57
58
59
60
61
62
63
64
65

5
6
7
8
9
10
11
12
13
14
15
16
17
18
19
20
21
22
23
24
25
26
27
28
29
30
31
32
33
34
35
36
37
38
39
40
41
42
43
44
45
46
47
48
49
50
51
52
53
54
55
56
57
58
59
60
61
62
63
64
65
14. J. Han, M. J. Hendzel and J. Allalunis-Turner, Quantitative analysis reveals asynchronous and more than DSB-associated histone H2AX phosphorylation after exposure to ionizing radiation. *Radiat Res* **165**, 283-292 (2006).

15. K. J. McManus and M. J. Hendzel, ATM-dependent DNA damage-independent mitotic phosphorylation of H2AX in normally growing mammalian cells. *Mol Biol Cell* **16**, 5013-5025 (2005).

16. J. Essers, W. A. van Cappellen, A. F. Theil, E. van Drunen, N. G. Jaspers, J. H. Hoeijmakers, C. Wyman, W. Vermeulen and R. Kanaar, Dynamics of relative chromosome position during the cell cycle. *Mol Biol Cell* **16**, 769-775 (2005).

17. S. H. MacPhail, J. P. Banath, Y. Yu, E. Chu and P. L. Olive, Cell cycle-dependent expression of phosphorylated histone H2AX: reduced expression in unirradiated but not X-irradiated G1-phase cells. *Radiat Res* **159**, 759-767 (2003).

18. A. Kinner, W. Wu, C. Staudt and G. Iliakis, Gamma-H2AX in recognition and signaling of DNA double-strand breaks in the context of chromatin. *Nucleic Acids Res* **36**, 5678-5694 (2008).

19. M. K. Whalen, S. K. Gurai, H. Zahed-Kargaran and J. M. Pluth, Specific ATM-mediated phosphorylation dependent on radiation quality. *Radiat Res* **170**, 353-364 (2008).

20. A. Forand, B. Dutrillaux and J. Bernardino-Sgherri, Gamma-H2AX expression pattern in non-irradiated neonatal mouse germ cells and after low-dose gamma-radiation: relationships between chromatid breaks and DNA double-strand breaks. *Biol Reprod* **71**, 643-649 (2004).

21. E. Soutoglou and T. Misteli, Activation of the Cellular DNA Damage Response in the Absence of DNA Lesions. *Science* (2008).

22. S. H. MacPhail, J. P. Banath, T. Y. Yu, E. H. Chu, H. Lambur and P. L. Olive, Expression of phosphorylated histone H2AX in cultured cell lines following exposure to X-rays. *Int J Radiat Biol* **79**, 351-358 (2003).

23. H. Wang, Z. C. Zeng, T. A. Bui, E. Sonoda, M. Takata, S. Takeda and G. Iliakis, Efficient rejoining of radiation-induced DNA double-strand breaks in vertebrate cells deficient in genes of the RAD52 epistasis group. *Oncogene* **20**, 2212-2224 (2001).

24. B. Stenerlow, K. H. Karlsson, B. Cooper and B. Rydberg, Measurement of prompt DNA double-strand breaks in mammalian cells without including heat-labile sites: results for cells deficient in nonhomologous end joining. *Radiat Res* **159**, 502-510 (2003).

25. S. V. Costes, A. Ponomarev, J. L. Chen, D. Nguyen, F. A. Cucinotta and M. H. Barcellos-Hoff, Image-based modeling reveals dynamic redistribution of DNA damage into nuclear sub-domains. *PLoS Comput Biol* **3**, e155 (2007).

26. E. L. Leatherbarrow, J. V. Harper, F. A. Cucinotta and P. O'Neill, Induction and quantification of gamma-H2AX foci following low and high LET-irradiation. *Int J Radiat Biol* **82**, 111-118 (2006).

27. T. A. Kato, R. Okayasu and J. S. Bedford, Comparison of the induction and disappearance of DNA double strand breaks and gamma-H2AX foci after irradiation of chromosomes in G1-phase or in condensed metaphase cells. *Mutat Res* **639**, 108-112 (2008).

5
6
7
8
9
10
11
12
13
14
15
16
17
18
19
20
21
22
23
24
25
26
27
28
29
30
31
32
33
34
35
36
37
38
39
40
41
42
43
44
45
46
47
48
49
50
51
52
53
54
55
56
57
58
59
60
61
62
63
64
65
28. K. Rothkamm and M. Lobrich, Evidence for a lack of DNA double-strand break repair in human cells exposed to very low x-ray doses. *Proc Natl Acad Sci U S A* **100**, 5057-5062 (2003).

29. A. Asaithamby and D. J. Chen, Cellular responses to DNA double-strand breaks after low-dose gamma-irradiation. *Nucleic Acids Res* **37**, 3912-3923 (2009).

30. H. Mahrhofer, S. Burger, U. Oppitz, M. Flentje and C. S. Djuzenova, Radiation induced DNA damage and damage repair in human tumor and fibroblast cell lines assessed by histone H2AX phosphorylation. *Int J Radiat Oncol Biol Phys* **64**, 573-580 (2006).

31. T. Tanaka, A. Kurose, X. Huang, F. Traganos, W. Dai and Z. Darzynkiewicz, Extent of constitutive histone H2AX phosphorylation on Ser-139 varies in cells with different TP53 status. *Cell Prolif* **39**, 313-323 (2006).

32. J. Bewersdorf, B. T. Bennett and K. L. Knight, H2AX chromatin structures and their response to DNA damage revealed by 4Pi microscopy. *Proc Natl Acad Sci U S A* **103**, 18137-18142 (2006).

33. H. Nikjoo, P. O'Neill, D. T. Goodhead and M. Terrissol, Computational modelling of low-energy electron-induced DNA damage by early physical and chemical events. *Int J Radiat Biol* **71**, 467-483 (1997).

34. H. Nikjoo, P. O'Neill, W. E. Wilson and D. T. Goodhead, Computational approach for determining the spectrum of DNA damage induced by ionizing radiation. *Radiat Res* **156**, 577-583 (2001).

35. K. H. Karlsson and B. Stenerlow, Focus formation of DNA repair proteins in normal and repair-deficient cells irradiated with high-LET ions. *Radiat Res* **161**, 517-527 (2004).

36. B. Jakob, M. Scholz and G. Taucher-Scholz, Biological imaging of heavy charged-particle tracks. *Radiat Res* **159**, 676-684 (2003).

37. N. Desai, E. Davis, P. O'Neill, M. Durante, F. A. Cucinotta and H. Wu, Immunofluorescence detection of clustered gamma-H2AX foci induced by HZE-particle radiation. *Radiat Res* **164**, 518-522 (2005).

38. B. Stenerlow, E. Blomquist, E. Grusell, T. Hartman and J. Carlsson, Rejoining of DNA double-strand breaks induced by accelerated nitrogen ions. *Int J Radiat Biol* **70**, 413-420 (1996).

39. M. Lobrich, P. K. Cooper and B. Rydberg, Joining of correct and incorrect DNA ends at double-strand breaks produced by high-linear energy transfer radiation in human fibroblasts. *Radiat Res* **150**, 619-626 (1998).

40. B. Jakob, J. Splinter and G. Taucher-Scholz, Positional stability of damaged chromatin domains along radiation tracks in mammalian cells. *Radiat Res* **171**, 405-418 (2009).

41. O. Zgheib, Y. Huyen, R. A. DiTullio, Jr., A. Snyder, M. Venere, E. S. Stavridi and T. D. Halazonetis, ATM signaling and 53BP1. *Radiother Oncol* **76**, 119-122 (2005).

42. Y. Huyen, O. Zgheib, R. A. Ditullio, Jr., V. G. Gorgoulis, P. Zacharatos, T. J. Petty, E. A. Sheston, H. S. Mellert, E. S. Stavridi and T. D. Halazonetis, Methylated lysine 79 of histone H3 targets 53BP1 to DNA double-strand breaks. *Nature* **432**, 406-411 (2004).

5
6
7
8
9
10
11
12
13
14
15
16
17
18
19
20
21
22
23
24
25
26
27
28
29
30
31
32
33
34
35
36
37
38
39
40
41
42
43
44
45
46
47
48
49
50
51
52
53
54
55
56
57
58
59
60
61
62
63
64
65
43. S. Burma, B. P. Chen, M. Murphy, A. Kurimasa and D. J. Chen, ATM phosphorylates histone H2AX in response to DNA double-strand breaks. *J Biol Chem* **276**, 42462-42467 (2001).

44. J. A. Aten, J. Stap, P. M. Krawczyk, C. H. van Oven, R. A. Hoebe, J. Essers and R. Kanaar, Dynamics of DNA double-strand breaks revealed by clustering of damaged chromosome domains. *Science* **303**, 92-95 (2004).

45. N. F. Lowndes and G. W. Toh, DNA repair: the importance of phosphorylating histone H2AX. *Curr Biol* **15**, R99-R102 (2005).

46. I. G. Cowell, N. J. Sunter, P. B. Singh, C. A. Austin, B. W. Durkacz and M. J. Tilby, gammaH2AX Foci Form Preferentially in Euchromatin after Ionising-Radiation. *PLoS ONE* **2**, e1057 (2007).

47. T. C. Karagiannis, K. N. Harikrishnan and A. El-Osta, Disparity of histone deacetylase inhibition on repair of radiation-induced DNA damage on euchromatin and constitutive heterochromatin compartments. *Oncogene* **26**, 3963-3971 (2007).

48. R. L. Warters and B. W. Lyons, Variation in radiation-induced formation of DNA double-strand breaks as a function of chromatin structure. *Radiat Res* **130**, 309-318 (1992).

49. J. Nygren, M. Ljungman and G. Ahnstrom, Chromatin structure and radiation-induced DNA strand breaks in human cells: soluble scavengers and DNA-bound proteins offer a better protection against single- than double-strand breaks. *Int J Radiat Biol* **68**, 11-18 (1995).

50. A. Munshi, T. Tanaka, M. L. Hobbs, S. L. Tucker, V. M. Richon and R. E. Meyn, Vorinostat, a histone deacetylase inhibitor, enhances the response of human tumor cells to ionizing radiation through prolongation of gamma-H2AX foci. *Mol Cancer Ther* **5**, 1967-1974 (2006).

51. Y. Zhang, M. Adachi, H. Zou, M. Hareyama, K. Imai and Y. Shinomura, Histone deacetylase inhibitors enhance phosphorylation of histone H2AX after ionizing radiation. *Int J Radiat Oncol Biol Phys* **65**, 859-866 (2006).

52. K. Camphausen, W. Burgan, M. Cerra, K. A. Oswald, J. B. Trepel, M. J. Lee and P. J. Tofilon, Enhanced radiation-induced cell killing and prolongation of gammaH2AX foci expression by the histone deacetylase inhibitor MS-275. *Cancer Res* **64**, 316-321 (2004).

53. C. A. Banuelos, J. P. Banath, S. H. MacPhail, J. Zhao, T. Reitsema and P. L. Olive, Radiosensitization by the histone deacetylase inhibitor PCI-24781. *Clin Cancer Res* **13**, 6816-6826 (2007).

54. E. Soutoglou, J. F. Dorn, K. Sengupta, M. Jasin, A. Nussenzweig, T. Ried, G. Danuser and T. Misteli, Positional stability of single double-strand breaks in mammalian cells. *Nat Cell Biol* **9**, 675-682 (2007).

55. A. A. Goodarzi, A. T. Noon, D. Deckbar, Y. Ziv, Y. Shiloh, M. Lobrich and P. A. Jeggo, ATM signaling facilitates repair of DNA double-strand breaks associated with heterochromatin. *Mol Cell* **31**, 167-177 (2008).

56. A. A. Goodarzi, A. T. Noon and P. A. Jeggo, The impact of heterochromatin on DSB repair. *Biochem Soc Trans* **37**, 569-576 (2009).

57. J. P. Quivy, A. Gerard, A. J. Cook, D. Roche and G. Almouzni, The HP1-p150/CAF-1 interaction is required for pericentric heterochromatin replication and S-phase progression in mouse cells. *Nat Struct Mol Biol* **15**, 972-979 (2008).

58. T. Cremer and C. Cremer, Chromosome territories, nuclear architecture and gene regulation in mammalian cells. *Nat Rev Genet* **2**, 292-301 (2001).

59. C. H. Chuang, A. E. Carpenter, B. Fuchsova, T. Johnson, P. de Lanerolle and A. S. Belmont, Long-range directional movement of an interphase chromosome site. *Curr Biol* **16**, 825-831 (2006).

60. N. Ayoub, A. D. Jeyasekharan, J. A. Bernal and A. R. Venkitaraman, HP1-beta mobilization promotes chromatin changes that initiate the DNA damage response. *Nature* **453**, 682-686 (2008).

61. M. S. Luijsterburg, C. Dinant, H. Lans, J. Stap, E. Wiernasz, S. Lagerwerf, D. O. Warmerdam, M. Lindh, M. C. Brink, et al., Heterochromatin protein 1 is recruited to various types of DNA damage. *J Cell Biol* **185**, 577-586 (2009).

62. M. Zarebski, E. Wiernasz and J. W. Dobrucki, Recruitment of heterochromatin protein 1 to DNA repair sites. *Cytometry A* **75**, 619-625 (2009).

63. G. Obe, P. Pfeiffer, J. R. Savage, C. Johannes, W. Goedecke, P. Jeppesen, A. T. Natarajan, W. Martinez-Lopez, G. A. Folle and M. E. Drets, Chromosomal aberrations: formation, identification and distribution. *Mutat Res* **504**, 17-36 (2002).

64. S. M. Bailey and J. S. Bedford, Studies on chromosome aberration induction: what can they tell us about DNA repair? *DNA Repair (Amst)* **5**, 1171-1181 (2006).

65. M. Suzuki, K. Suzuki, S. Kodama and M. Watanabe, Interstitial chromatin alteration causes persistent p53 activation involved in the radiation-induced senescence-like growth arrest. *Biochem Biophys Res Commun* **340**, 145-150 (2006).

66. M. Suzuki, K. Suzuki, S. Kodama and M. Watanabe, Phosphorylated histone H2AX foci persist on rejoined mitotic chromosomes in normal human diploid cells exposed to ionizing radiation. *Radiat Res* **165**, 269-276 (2006).

67. E. Markova, N. Schultz and I. Y. Belyaev, Kinetics and dose-response of residual 53BP1/gamma-H2AX foci: co-localization, relationship with DSB repair and clonogenic survival. *Int J Radiat Biol* **83**, 319-329 (2007).

68. D. Klokov, S. M. MacPhail, J. P. Banath, J. P. Byrne and P. L. Olive, Phosphorylated histone H2AX in relation to cell survival in tumor cells and xenografts exposed to single and fractionated doses of X-rays. *Radiother Oncol* **80**, 223-229 (2006).

69. E. P. Rogakou, C. Boon, C. Redon and W. M. Bonner, Megabase chromatin domains involved in DNA double-strand breaks in vivo. *J Cell Biol* **146**, 905-916 (1999).

70. D. R. Pilch, O. A. Sedelnikova, C. Redon, A. Celeste, A. Nussenzweig and W. M. Bonner, Characteristics of gamma-H2AX foci at DNA double-strand break sites. *Biochem Cell Biol* **81**, 123-129 (2003).

71. S. Costes, R. Sachs, L. Hlatky, D. Vannais, C. Waldren and B. Fouladi, Large-mutation spectra induced at hemizygous loci by low-LET radiation: evidence for intrachromosomal proximity effects. *Radiat Res* **156**, 545-557 (2001).

72. J. B. Little, Radiation carcinogenesis. *Carcinogenesis* **21**, 397-404 (2000).

73. K. K. Khanna and S. P. Jackson, DNA double-strand breaks: signaling, repair and the cancer connection. *Nat Genet* **27**, 247-254 (2001).

74. T. Yu, S. H. MacPhail, J. P. Banath, D. Klokov and P. L. Olive, Endogenous expression of phosphorylated histone H2AX in tumors in relation to DNA double-strand breaks and genomic instability. *DNA Repair (Amst)* **5**, 935-946 (2006).

5
6
7
8
9
10
11
12
13
14
15
16
17
18
19
20
21
22
23
24
25
26
27
28
29
30
31
32
33
34
35
36
37
38
39
40
41
42
43
44
45
46
47
48
49
50
51
52
53
54
55
56
57
58
59
60
61
62
63
64
65
75. B. Jakob, J. Splinter, M. Durante and G. Taucher-Scholz, Live cell microscopy analysis of radiation-induced DNA double-strand break motion. *Proc Natl Acad Sci U S A* **106**, 3172-3177 (2009).

Figure1

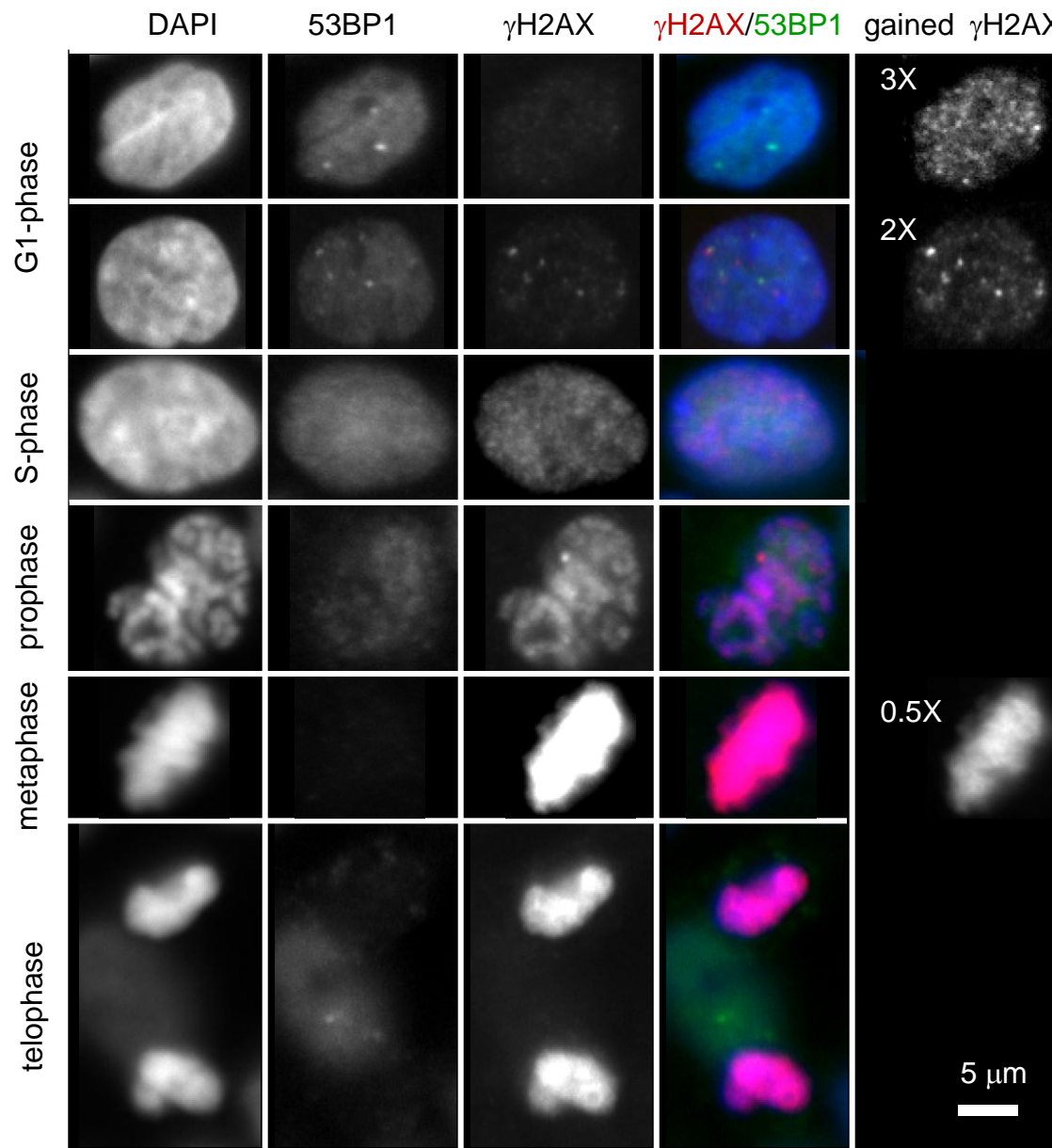


Figure2

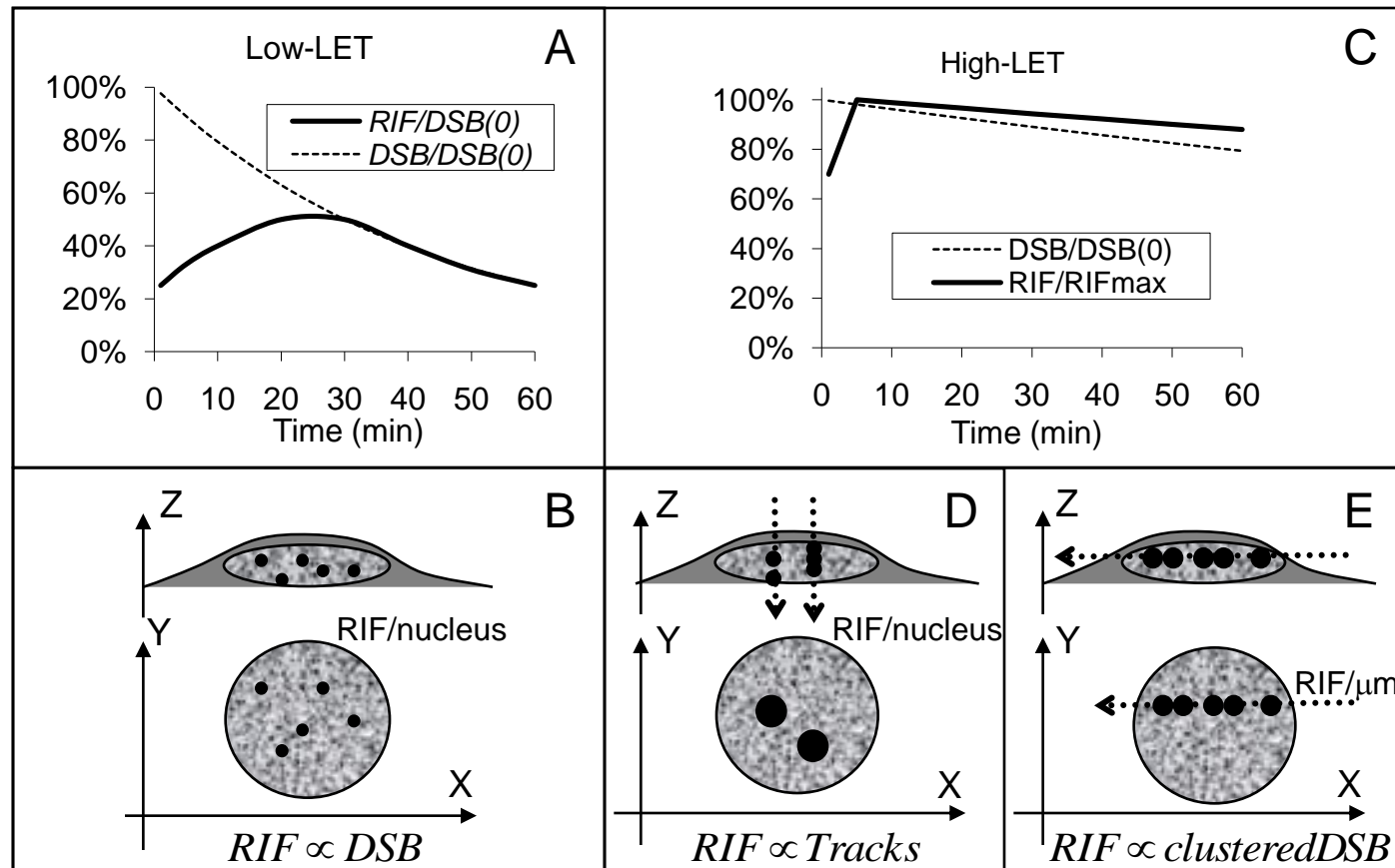


Figure3

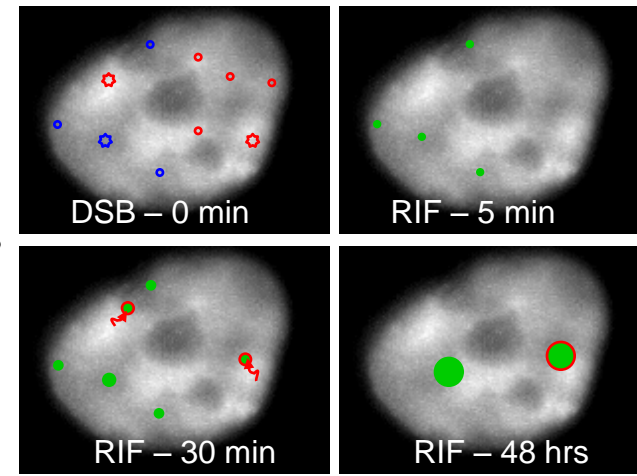
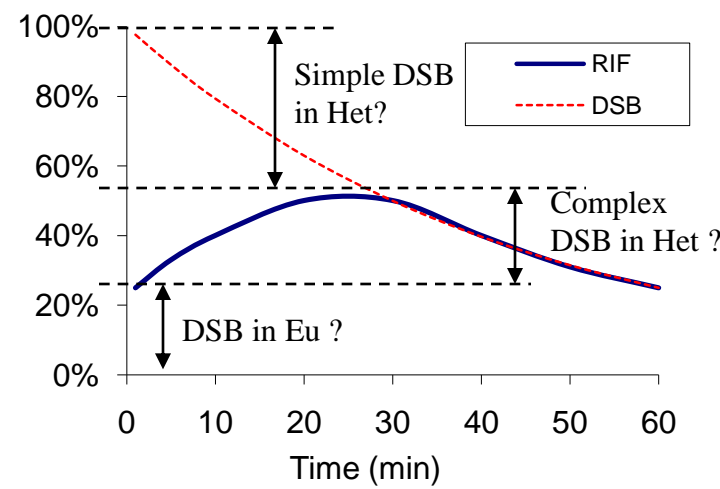


Figure4

